論文 / 著書情報
Article / Book Information

Title	Determination of LQR weights by Bayesian optimization method using multiple earthquake waves
Authors	Kou Miyamoto, Nobuaki Yasuo, Yinli Chen, Daiki Sato, Jinhua She
Citation	Proceedings of IEEE 46th Annual Conference of the IEEE Industrial Electronics Society(IECON2020), , , pp. 2651-2655
Pub. date	2020, 10
Copyright	(c) 2020 IEEE. Personal use of this material is permitted. Permission from IEEE must be obtained for all other uses, in any current or future media, including reprinting/republishing this material for advertising or promotional purposes, creating new collective works, for resale or redistribution to servers or lists, or reuse of any copyrighted component of this work in other works.
DOI	http://dx.doi.org/10.1109/IECON43393.2020.9254573
Note	This file is author (final) version.

Determination of LQR weights by Bayesian optimization method using multiple earthquake waves

Kou Miyamoto*, Nobuaki Yasuo#, Yinli Chen#, Daiki Sato# and Jinhua She$

* Shimizu Corporation, Koto, Tokyo 135-0044, Japan
# Tokyo Institute of Technology, Yokohama, Kanagawa 226-8503, Japan
$ Tokyo University of Technology, Hachioji, Tokyo 192-0982, Japan

***Abstract*— An active structural-control strategy has been widely studied to improve the control performance. Most studies used the linear quadratic-regulator (LQR) method to design the state-feedback controller. The LQR method requires to tune many weights in the cost function to design the controller. Moreover, various earthquake waves have to be considered. Thus, it is difficult to determine the weights. This paper determines the weights by using the Bayesian optimization method with multiple earthquake waves to reduces the burden of tuning the weights.**

***Index Terms*—Active structural control, LQR, Bayesian optimization method, parameter tuning**

I. Introduction

The active structural-control method has been studied rapidly in these few decades. Many control methods are applied to design the controller gain such as the classical control method, modern control theory, and some advanced control strategies. One of the most common methods is the linear quadratic-regulator (LQR) method [1]. The state-feedback controller is designed by minimizing the cost function that has the weighting matrices. Since the relationship between the weighting parameters and the control performance is complex, the trial-and-error method has been used to determine the controller gain [2]. In contrast, Fujitani et al. clarified the influence on the weights to the dynamic characteristics for the single degree-of-freedom (SDOF) models [3]. This study used the building model that does not have a damping factor. To solve this problem, Sato et al. extended this method to a building model with a damping factor and presented a new design spectrum [4].

These studies deal with the SDOF model, however, most buildings are modeled as the multi-DOF (MDOF) model. In recently, some studies consider a MDOF models. For example, Kohiyama et al. presented a method that estimates the responses for the MDOF model by using the complex-complete-quadratic-combination (CCQC) method [5]. Elumalai et al. have shown the weighting matrices can be yielded by solving the inverse problem for MDOF models [6]. However, if a building model is high-DOF system, many damping ratios and natural frequencies have to be chosen to calculate the weighting matrices. To solve these problems, the Bayesian optimization (BO) method is applied. This method is one of the nonparametric optimization methods, and it estimates the relationship between the input and output by using the Gaussian process [8].

Marco et al. applied the BO method to determine the LQR weighting matrices and Miyamoto et al. extended this method for tuning active structural-control systems [9,10].

Miyamoto et al. used the BO method to determine the weighting matrices (AD-LQR method), considering not only the displacement, but also the absolute acceleration and the inter-story drifts and velocities [10]. In this study, only one artificial wave was used to find the weights. However, the dominant frequency is different for different earthquake wave and several waves have to be considered to design the state-feedback controller.

This paper presents a new BO method that determines the weighting matrices using multiple earthquake waves. The numerical example uses the 11-DOF base-isolated building model.

II. Building dynamics and LQR Method

The dynamics of the building model is

$$M_S\ddot{x}(t)+D_S\dot{x}(t)+K_S x(t)=-M_S E_d\ddot{x}_g(t)+E_u u(t) \tag{1}$$

where M_S is the mass matrix, D_S is the damping matrix, K_S is the stiffness matrix, E_d is the disturbance input matrix, E_u is the control input matrix, $x(t)$ is the displacement vector, and the $x_g(t)$ is the displacement of the ground.

The state space representation of (1) is shown in

$$\dot{z}(t)=Az(t)+Bu(t)+B_d d(t) \tag{2}$$

where

$$\begin{cases} z(t)=\begin{bmatrix} x(t) \\ \dot{x}(t) \end{bmatrix}, & A=\begin{bmatrix} 0 & 1 \\ -M_S K_S^{-1} & -M_S D_S^{-1} \end{bmatrix} \\ B_d=\begin{bmatrix} 0 \\ M_S E_d \end{bmatrix}, & B_u=\begin{bmatrix} 0 \\ M_S E_u \end{bmatrix}. \end{cases} \tag{3}$$

The state consists of the relative displacement and the relative velocity of the building.

The block diagram of the control system, (2), is described in Fig. 1.

The state-feedback controller is designed by the LQR method. The LQR method determines the state-feedback controller by minimizing the following cost function J:

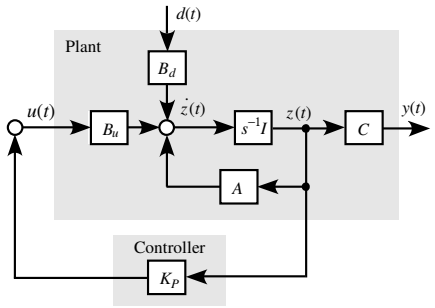

Figure 1. Block diagram of state-feedback control system

$$J=\int_0^\infty \left\{\begin{bmatrix}\Delta x(t) & \Delta\dot{x}(t)\end{bmatrix}^{\mathrm{T}} Q_d \begin{bmatrix}\Delta x(t)\\ \Delta\dot{x}(t)\end{bmatrix} + \left[\ddot{x}(t)+\ddot{x}_g(t)\right]^{\mathrm{T}} Q_g \left[\ddot{x}(t)+\ddot{x}_g(t)\right] + u^{\mathrm{T}}(t)R_u u(t)\right\}dt, \tag{4}$$

where Q_d (>0) and Q_g (>0) are the weighting matrices for these responses and $\Delta x(t)$ is the inter-story drift vector, which is given by

$$\begin{cases}\begin{bmatrix}\Delta x(t)\\ \Delta\dot{x}(t)\end{bmatrix}=\begin{bmatrix}\Gamma & \\ & \Gamma\end{bmatrix}\begin{bmatrix}x(t)\\ \dot{x}(t)\end{bmatrix}\\ \Gamma=\begin{bmatrix}1 & & & \\ -1 & 1 & & \\ \vdots & & \ddots & \\ 0 & \cdots & -1 & 1\end{bmatrix}.\end{cases} \tag{5}$$

Regrouping the equation of motion, (1), gives

$$\ddot{x}(t)+\ddot{x}_g(t)=\Xi\, z(t)+\Psi u(t), \tag{6}$$

where $\Xi=\begin{bmatrix}-M^{-1}K & -M^{-1}D\end{bmatrix}$ and $\Psi=-M^{-1}E_u$,

Substituting (5) and (6) into (4) yields

$$J=\int_0^\infty \left\{z^{\mathrm{T}}(t)Qz(t)+2z(t)Su(t)+u^{\mathrm{T}}(t)Ru(t)\right\}dt \tag{7}$$

where

$$\begin{cases}Q=\Gamma Q_d\Gamma+\Xi^{\mathrm{T}}Q_g\Xi\mathrm{a}\\ 2z(t)Su(t)=-z^{\mathrm{T}}(t)\Xi^{\mathrm{T}}Q_g\Psi u(t)+u^{\mathrm{T}}(t)\Psi^{\mathrm{T}}Q_g\Xi z(t).\\ R=\Psi^{\mathrm{T}}Q_g\Psi+R_u\end{cases} \tag{8}$$

The state-feedback controller, K_p, is given by

$$K_P=-R^{-1}\left(S^{\mathrm{T}}+B_{\mathrm{u}}^{\mathrm{T}}P\right), \tag{9}$$

where P (> 0) is the solution of the Riccati equation:

$$\begin{aligned}&\left(A-B_uR^{-1}S^{\mathrm{T}}\right)^{\mathrm{T}}P+P\left(A-B_uR^{-1}S^{\mathrm{T}}\right)\\ &+Q-PB_uR^{-1}B_u^{\mathrm{T}}P-SR^{-1}S^{\mathrm{T}}=0\end{aligned}. \tag{10}$$

III. Selecting Weights using Bayesian Optimization Method

This section explains the Bayesian optimization method and formulates the optimization problem for selecting weighting matrices.

3.1. Optimization problem of weights selection for one earthquake wave

The state-feedback controller, K_p, is described by using the parameters A, B, Q_d, Q_g and R :

$$K_p=LQR(A,\ B,\ Q_d,\ Q_g,\ R). \tag{11}$$

The controller gain, K_p, can be shown by using the vector θ to formulate the optimization problem:

$$K_p(\theta)=LQR(A,\ B,\ W_d(\theta),\ W_g(\theta),\ R). \tag{12}$$

where $W_d(\theta)$ and $W_g(\theta)$ are positive symmetric matrices, and the BO method searches θ by minimizing the objective function that is described in section 3.2.

The previous optimization problem is set as follows [9]:

$$\begin{aligned}&\arg\min_{\theta\in R^n}\ {}_{\max}A_C(\theta)=(A,B,K_p(\theta))\\ &s.t.\ \ {}_{\max}D_0(\theta)<{}_aD_0,\end{aligned} \tag{13}$$

where $A_C(\theta)$ and ${}_{\max}D_0(\theta)$ are the maximum absolute acceleration and displacement for the vector, θ, and ${}_aD_0$ is the allowable displacement for an earthquake wave.

3.2. Optimization problem of weights for multiple waves

Equation (13) searches the weights by using only one earthquake wave. However, as already stated before, the dominant frequency is different for each earthquake wave. Thus, many waves have to be considered to design the controller.

To take into account the influence of the multiple waves, this paper presents the following objective function:

$$\begin{aligned}&\arg\min_{\theta\in R^n}\ A_C(\theta)=\frac{1}{n}\sum_{i=1}^{n}\frac{A_{C,i}(\theta)}{A_{NC,i}}\\ &\text{s.t.}\ \ \forall i\ \ \max D_{0,i}(\theta)<{}_aD_0,\end{aligned}. \tag{14}$$

where $A_{C,i}$ (θ) and $A_{NC,i}$ are the maximum absolute acceleration for a building model with and without active structural controller, and ${}_{\max}D_{0,i}(\theta)$ is the maximum inter-story displacement for the i-th earthquake wave.

3.3. Gaussian process and model estimation

If a process follows the Gaussian distribution, then the process is defined as the Gaussian process (GPs).

The relationship between the weights, θ, and the response of the building is modeled and estimated by the GPs in this paper.

The estimated value of $A_c(\theta)$, $\tilde{A}_C(\theta)$, is described by

$$\tilde{A}_C(\theta)=A_C(\theta)+\varepsilon. \tag{15}$$

where $\varepsilon \sim N(0,\ \sigma_\varepsilon^2)$ is a Gaussian noise, and $N(0,\ \sigma_\varepsilon^2)$ is a Gaussian distribution with the average and variance are 0 and σ_ε^2. This paper estimates $\tilde{A}_C(\theta)$ by using the Gaussian process. If a process $f(\theta)$ follows the Gaussian process it is expressed by

$$f(\theta)\sim GP(\mu_f(\theta),\ \ K_C(\theta,\theta')), \tag{16}$$

where μ_f is the mean function and K_C is the covariance.

The mean function and a covariance matrix determine the characteristics of the GP. In (16), $\mu_f(\theta)$ can be chosen to be 0, θ' is an arbitrary input, and K_C is given by

$$K_C(\theta,\theta')=\sigma_f^2\exp\left(-\frac{1}{2}(\theta-\theta')^{\mathrm{T}}\Sigma^{-1}(\theta-\theta')\right) \tag{17}$$

where σ_f^2 is the prior variance of $f(\theta)$ and Σ is a variance-covariance matrix.

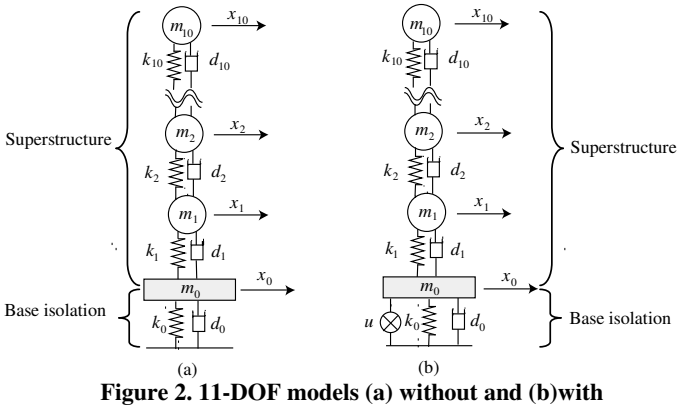

Figure 2. 11-DOF models (a) without and (b)with active structural control device

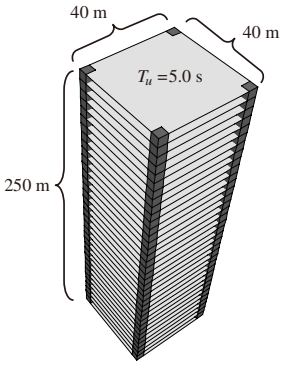

Figure 3. Building model

An input vector $\theta_* = [\theta_{*1},...,\theta_{*n}]$, which is selected by the BO method, is used for training; and the output of the vector, $A_C(\theta_*) = [A_C(\theta_{*1}),...,A_C(\theta_{*n})]$, is set to calculate the prior average and variance of the objective function, $A_c(\theta)$. The estimated Gaussian distribution is described as

$$p(\tilde{A}_C(\theta_*) \mid \Phi, \theta) \sim N(\mu(\theta_*),\ \sigma^2(\theta_*)), \tag{18}$$

where $\Phi = \{\theta_*,\ A_C(\theta_*)\}$ is a data set. The mean function, $\mu(\theta_*)$, and variance, $\sigma^2(\theta_*)$, are given by

$$\sigma(\theta_*) = K_C(\theta_*,\theta_*) - K_C(\theta_*,\theta)\{K_C(\theta,\theta) + \sigma_f^2 I\}K_C(\theta,\theta_*) \tag{19}$$

and

$$\mu(\theta_*) = K_C(\theta_*,\theta)\{K_C(\theta,\theta) + \sigma_f^2 I\}\tilde{A}_C(\theta_*). \tag{20}$$

3.4. Bayesian optimization

Bayesian optimization searches a global optimum value without calculating the gradient of an objective function. Explicit objective function or its gradient are not required to calculate an optimal value.

This optimization method iteratively renews the estimation of $\tilde{A}_C(\theta_{\text{new}})$ by updating the parameter, θ_{new}, and the objective function, $A_C(\theta_{\text{new}})$. The updated point, θ_{new}, is obtained by maximizing the following acquisition function, $\alpha(\theta_{\text{new}})$:

$$\theta_{\text{new}} = \arg\max\ \alpha(\theta_*). \tag{21}$$

The following probability of improvement of the objective function as the acquisition function:

$$\alpha(\theta) = E_\rho[\max(0,\ \mu_\rho(\theta_{best}) - \tilde{A}_C(\theta)]. \tag{22}$$

where $\mu_\rho(\theta)$ is the mean function of the posterior distribution, θ_{best} is the location that optimizes the objective function, and $\mu_\rho(\theta_{best})$ is the average of θ_{best}.

IV. Numerical Example

4.1 Building model

This section shows the numerical example and compares with the previous and new BO method. This paper uses the base isolated building, which is a 250 m high. The building is modeled as the 10-DOF shear building model and the base isolation is described by using the linear spring and viscous damper. The active structural controller is located in the base isolated story.

The parameters of the building model are shown as follows:

Density of passive base-isolation story: 2551 kg/m^2
Damping for passive base-isolation period (ζ_0)**:** 0.05
Area of building: 40 m×40 m
Natural first mode period of superstructure (T_u)**:** 5.0 s
Density of superstructure (for all stories): 175 kg/m^3
Height of superstructure (h_u)**:** = T_u/0.02 m
Each story height of superstructure (h_i)**:** = h_u/10 m
Damping of superstructure: Stiffness-proportional damping model (damping ratio for the first mode is assumed to be 0.02)
Stiffness of superstructure: Stiffness of the i-th story is

$$\begin{cases} k_i = \dfrac{\omega^2 \cdot m_i \cdot \phi_i + k_{i+1}(\phi_{i+1} - \phi_i)}{\phi_i - \phi_{i-1}}, & i = 2,...,9, \\ k_1 = \dfrac{\omega^2 \cdot m_1 \cdot \phi_1 + k_2(\phi_2 - \phi_1)}{\phi_1}, & k_{10} = \dfrac{\omega^2 \cdot m_{10} \cdot \phi_{10}}{\phi_{10} - \phi_9} \end{cases} \tag{23}$$

where ω is the first natural circular frequency; and for the i-th story (i = 0, 1, ..., 10), ϕ_i is the first mode and m_i is the mass for i-th story, which is given by the area of superstructure, each story height and the density of the superstructure. In this paper, the straight-line mode is used as the first mode to design the stiffness of each story.

The mass of the base isolated story is given by the product of the density and the area of the base isolated story. A laminated rubber in the base isolated story is modeled a linear spring and the viscous damper is modeled as a linear dashpot because of using the LQR method, which is the linear control strategy. The stiffness, k_0, and the damping coefficient, d_0, of the base isolated story are

$$k_0 = \frac{T_0^2}{4\pi^2(M_S + m_0)} \tag{24}$$

$$d_0 = 2\xi_0\sqrt{(M_S + m_0)k_0}. \tag{25}$$

where T_0 (= 8.0 s) is the period of the base isolated story with the building is assumed to be a rigid body, and M_S is the total mass of the superstructure.

4.2 Earthquake wave

The following three waves to design the controller:

1. Art Hachinohe wave: the spectrum of the pseudo velocity response, ${}_pS_v$, is 100 cm/s after a corner period of 0.64 s for a building with the damping ratio of 5%, and the phase characteristic is the same as those of the earthquake wave of Hachinohe EW 1968.

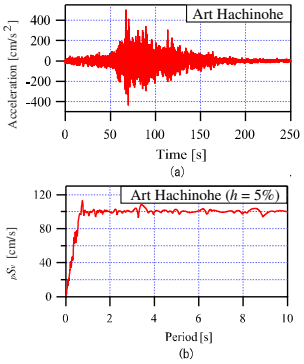

Figure 4.Art Hachinohe wave
(a) accelerogram
(b) pseud velocity response

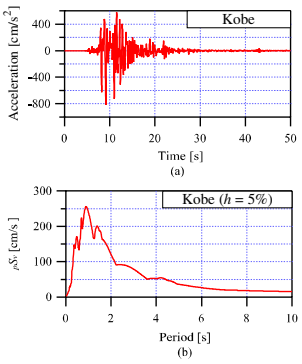

Figure 5. Kobe wave
(a) accelerogram
(b) pseud velocity response

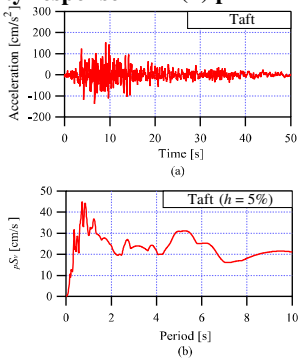

Figure 6. Taft wave: (a) accelerogram and (b) pseud velocity response

2. Kobe wave: JMA Kobe 1995, and
3. Taft wave: Taft NS 1952

Figure 4 shows that the velocity response for the Art Hachinohe wave is very large and it is 100 cm/s. Figures 5 and 6 show that the high frequency is dominant for the Kobe wave and low frequency is dominant for the Taft wave. This paper designes the state-feedback controller using the combination of these erathquake waves.

The following two waves are used to verify of our method:

・Shinjuku wave: The Niigata-ken Chuetsu-oki Earthquake (2007), at Shinjuku NS, and

・Kushiro wave: Tokachi-oki earthquake (2003) at Kushiro EW.

The accelerogram and the pseudo response spectrum are shown in Figs. 7 and 8.

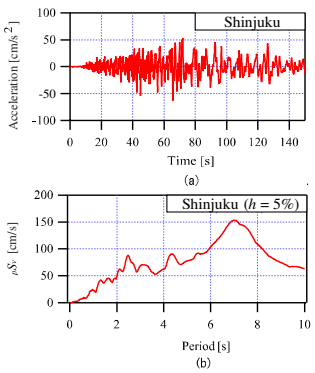

Figure 7 Shinjuku wave: (a) accelerogram and (b) pseud velocity response

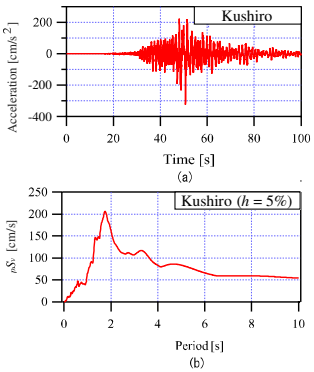

Figure 8 Kushiro wave: (a) accelerogram and (b) pseud velocity response

4.3 Simulation results

The weighting matrices are defined as equation (26):

$$\begin{cases} Q_d = 10^{diag\{q_{d1} \quad q_{d2} \quad \cdots \quad q_{d22}\}} I \\ Q_g = 10^{diag\{q_{g1} \quad q_{g2} \quad \cdots \quad q_{g11}\}} I. \end{cases} \tag{26}$$

Q_d is for the inter-story drift (q_{d1} ~ q_{d11}) and the velocity (q_{d12} ~ q_{d22}), and Q_g is for the absolute acceleration for each story. Note that the constraint of the optimization is set at the displacement of the base-isolated story, and the allowable range is set as 55 cm.

The control systems are assessed by using the Shinjuku and Kurhiro waves. The maximum displacement, inter-story drift and the maximum absolute acceleration are evaluated. Figures 9-14 show the results of the simulation. In these figures,

・K: the controller designed by using the Kobe wave.
・T: the controller designed by using the Taft wave.
・A: the controller designed by using the Art Hachinohe.
・A_K: the controller designed by using the Art Hachinohe and the Kobe waves.
・A_T: the controller designed by using the Art Hachinohe and Taft waves.
・K_T: the controller designed by using the Kobe and the Taft waves.
・A_K_T: the controller designed by using the Art Hachinohe, Kobe and the Taft waves.
・NC is the building without a controller.

Figures 9-11 show that if the controller is designed by considering the Taft wave, the maximum inter-story drift and the maximum absolute acceleration can be more suppressed than the other controllers against the Shinjuku wave. However, Figures 12-14 show that, if the controller is designed by using the Taft wave, the maximum displacement is very large, and the base isolated story is 140 cm beyond the allowable range, 55 cm. Moreover, the control performance of NC is better against Kushiro wave.

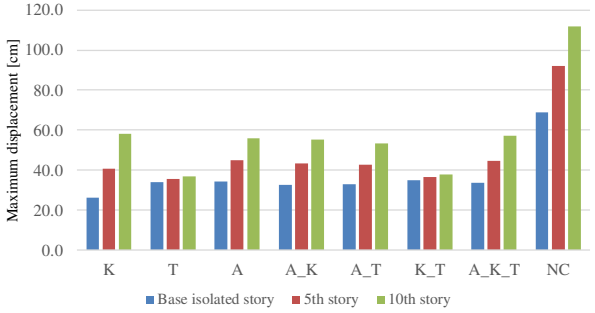

Figure 9. Maximum displacement for Shinjuku wave

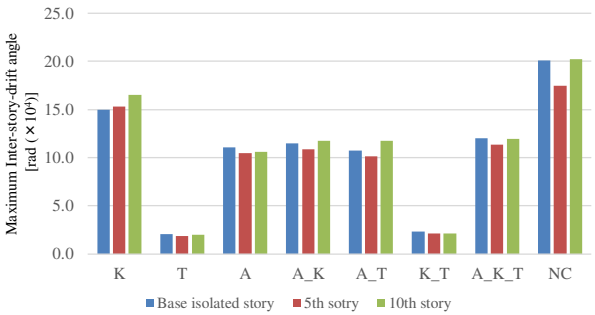

Figure 10. Maximum inter-story drift for Shinjuku wave

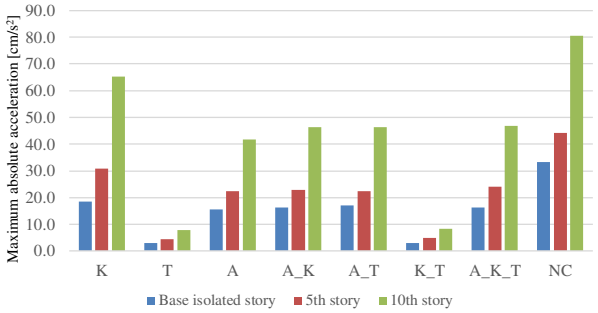

Figure 11. Maximum absolute acceleration for Shinjuku wave

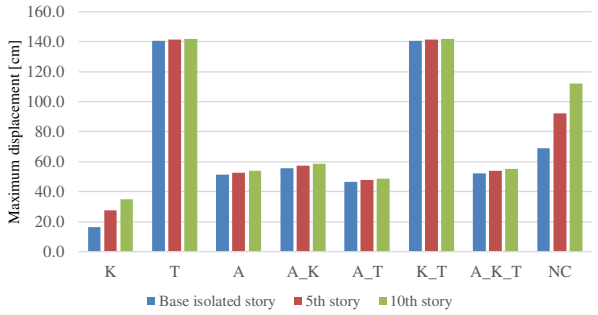

Figure 12. Maximum displacement for Kushiro wave

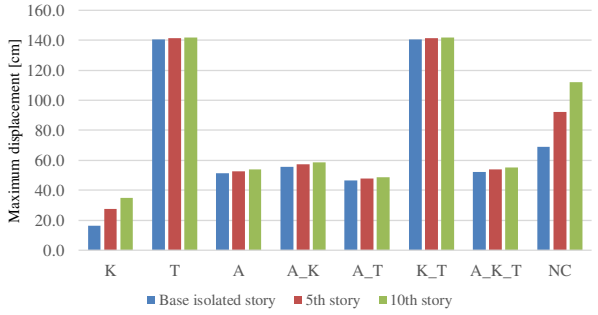

Figure 13. Maximum inter-story drift angle for Kushiro wave

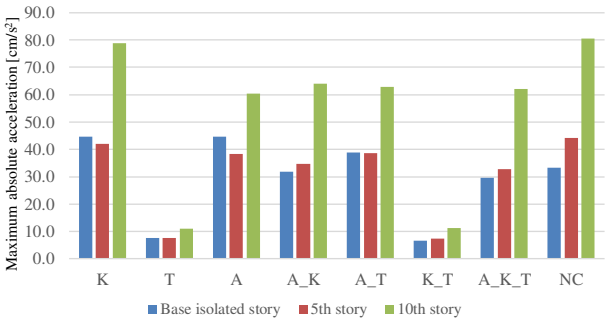

Figure 14. Maximum absolute acceleration for Kushiro wave

The previous BO method considers only one wave. However, it is may not enough to suppress various earthquake waves. A_K_T model, which considers multiple earthquake waves, performs better against both Shinjuku and Kushiro waves.

V. Conclusion

This study presented a new Bayesian optimization (BO) method, which consideres various earthquake waves, to select weigting matrices of LQR controllers. The 11 degree-of-freedom model with base isolation and five kinds of earthquake waves are used to verify our method. The simulation results show that if only one earthquake wave is taken into account in the optimization method, it may not be enough to suppress the responses for the various earthquake waves. On the other hand, our method considers multiple earthquake waves to select the weights at the same time, and it suppressses the responses of the control system for the different dominant frequency waves.

References

[1] Gawronsk W. K. : Advanced structural dynamics and active control of structures, Springer, 2004.

[2] Preumont A. and Seto K: Active control of structures, WILEY, 2008.

[3] Fujii H, Hiwatashi T., and Fujitani H. : Performance evaluation of semi-active optimzal control system by MR dampe: Evaluation of system performance of semi-active optimal contraol system and control parameter determination. *Journal of Structural and Construction Engineering (Transactions of AIJ)*, Vol. 72(618), pp. 73-79, 2008. (In Japanese)

[4] Sato D., Chen Y., Miyamoto K., and She J. : A spectrum for estimating the maximum control force for passive-base-isolated buildings with LQR control, *Engineering Structures*, Vol. 199 (15), 2019.

[5] Ishizawa Y. and Kohiyama M. : Maximum response estimation of a mid-story isolated building based on complex complete quadratic combination *method considering mode-dependent peak factors, Theoretical and Applied Mechanics Japan,* Vol. 63, 2015.

[6] *V. K. Elumalai and R. G. Subramanian. : A new algebraic LQR weight selection algorithm for tracking control of 2 DoF torsion system, Archives of Electrical Engineering,* Vol. 66(1), 2017.

[7] *Mockus J. On Bayesian methods for seeking the extremum, In Proc. IFIP Technical Conference* 1974: 400–404.

[8] *Marco A., Hennig P., Bohg J., Schaal S., and Trimpe S.: Automatic LQR Tuning Based on Gaussian Process Global* Optimization, *IEEE 2016 International Conference on Robotics and Automation*, 2016.

[9] Miyamoto K., She J., Sato D., and Yasuo N.: Automatic determination of LQR weighting matrices for active structural control, *Engineering Structures*, Vol. 174 (1), 2018.